ADVANCING EARTH AND SPACE SCIENCES

Geophysical Research Letters

RESEARCH LETTER

10.1029/2026GL122843

# Mass Loss From Thwaites Glacier Continues Even Without Ocean Melting

C. Rosie Williams[1], Matt Trevers[2], Sainan Sun[3], Paul R. Holland[1], David T. Bett[1], Robert J. Arthern[1], and Alexander T. Bradley[4]

[1]British Antarctic Survey, Cambridge, UK, [2]University of Bristol, Bristol, UK, [3]University of Northumbria, Newcastle, UK, [4]King's College London, London, UK

**Key Points:**

- Drivers of ongoing ice loss from Pine Island and Thwaites glaciers are assessed by removing all ocean melting in three ice-sheet models
- Pine Island Glacier responds by thickening and advancing, but Thwaites continues to lose ice, at a decaying rate
- Thwaites is responding to a historical perturbation and ocean cooling alone cannot reverse historical ice loss over centennial timescales

**Supporting Information:**

Supporting Information may be found in the online version of this article.

**Correspondence to:**

C. R. Williams,
chll1@bas.ac.uk

**Citation:**

Williams, C. R., Trevers, M., Sun, S., Holland, P. R., Bett, D. T., Arthern, R. J., & Bradley, A. T. (2026). Mass loss from Thwaites Glacier continues even without ocean melting. *Geophysical Research Letters*, *53*, e2026GL122843. https://doi.org/10.1029/2026GL122843

Received 7 MAR 2026
Accepted 16 JUL 2026

**Abstract** Pine Island and Thwaites glaciers dominate Antarctica's sea-level contribution. However, it remains unclear whether their ice loss is driven by anomalously warm present-day ocean conditions, perhaps linked to anthropogenic climate change, or are an ongoing response to historical natural climate anomalies. Here, we probe these drivers by subjecting three state-of-the-art ice-sheet models to an extreme hypothetical scenario of zero ocean melting. Pine Island responds by thickening and re-advancing to the prominent seabed ridge on which it was grounded prior to 1940. In contrast, Thwaites continues to lose ice (at a decreasing rate) for 150 years, despite the absence of ocean melting. Since all present-day ocean forcing via melt is removed, this demonstrates that the ongoing Thwaites ice loss is at least partly supported by the response to a historical perturbation. It also demonstrates that Thwaites' present-day mass loss trend cannot be reversed by ocean cooling alone, over policy-relevant centennial timescales.

**Plain Language Summary** Pine Island and Thwaites glaciers in West Antarctica are losing ice and contributing to global sea-level rise. Ocean-driven melting beneath their floating ice shelves can cause the glaciers to thin and retreat inland, but it remains unclear what is driving today's ice loss. One possibility is that previous natural periods of unusually warm ocean conditions, such as occurred the 1940s, caused the glaciers to retreat inland, and they are still adjusting to such events. Another possibility is that ongoing warm ocean conditions continue to drive retreat, perhaps linked to human-induced climate change. To separate these effects, we conducted an extreme modeling experiment in which we removed all ocean melting in three state-of-the-art numerical ice-sheet models. When ocean forcing is removed Pine Island Glacier thickens and advances toward its pre-1940s position, as might be expected. In contrast, Thwaites Glacier continues to lose ice over 150 years despite the absence of any ocean melting. This shows that Thwaites is responding to a historical climate disturbance, which has triggered a phase of ice loss that continues irrespective of present melting. The results also demonstrate that ocean cooling measures alone may not be sufficient to recover the historical Thwaites Glacier state over centennial timescales.

## 1. Introduction

The West Antarctic Ice Sheet contains enough ice to raise global sea levels by ~5 m (Morlighem et al., 2020) and is losing ice at an accelerating rate (Shepherd et al., 2019). The Amundsen Sea Embayment, containing Pine Island Glacier (PIG) and Thwaites Glacier (TG), is the dominant source of ice loss (Rignot et al., 2019; Smith et al., 2020). Sub-ice shelf sediment records show synchronous retreat of these glaciers starting in the mid-twentieth century, with PIG ungrounding from a submarine ridge and TG from its Western pinning point in the 1940/50s (Clark et al., 2024; Shepherd et al., 2004; Smith et al., 2017).

Despite this synchronicity, PIG and TG's geometries and ice-shelf stress regimes are distinctly different. PIG has a narrow, confined main trunk flowing into an ice shelf with relatively strong shear margins (Mouginot et al., 2014). TG has a wider grounding zone flowing into the Thwaites Western Ice Tongue (TWIT) and Thwaites Eastern Ice Shelf (TEIS), which decoupled in 2006–2007 when TWIT disintegrated into a melange of icebergs (Alley et al., 2021; Mouginot et al., 2014). Modeling studies suggest that PIG's ice shelf exerts a significant resistive back stress to the upstream flow (known as buttressing) while TG's ice shelf does not (Gudmundsson et al., 2023). However, this does not imply that ocean melting has no influence on TG; if melting were to decrease, the ice could thicken and re-ground, providing enhanced buttressing to the upstream glacier. During future retreat, ocean melting can also affect the rate of ice loss: the rate of melting around small pinning points formed during the retreat of TG can exert a large control on the rate of sea-level rise (Bett et al., 2024).

The ice loss in this sector is ultimately caused by changes in ocean melting (Mawbey et al., 2026; Shepherd et al., 2004) but it remains unclear the extent to which the ice loss reflects any of (a) the ongoing response to anomalously warm present-day ocean conditions, potentially caused by anthropogenic climate change (Holland et al., 2019; Naughten et al., 2022, 2023); (b) a decaying response to a strong climatic anomaly in the 1940s that displaced the glaciers from their seabed ridges, the consequences of which are still unfolding (Holland et al., 2022; O'Connor et al., 2023; Steig et al., 2012); and/or (c) the activation of self-reinforcing feedbacks that may continue to amplify ice loss over coming centuries. Such feedbacks could involve acceleration due to ice damage (Lhermitte et al., 2020) and geometry changes (Joughin et al., 2014), and increased melting due to freshwater fluxes (Bett et al., 2020) and cavity geometry (Holland et al., 2023).

In this study, we probe these three drivers of ice loss by completely removing the present-day ocean forcing, thus exposing the role of historical perturbations and ongoing ocean melt. We use three state-of-the-art ice sheet models (Gudmundsson et al., 2023; Trevers et al., 2024; Williams et al., 2025) to simulate the response of PIG and TG in an extreme hypothetical scenario of zero ocean melting, maintained over a policy-relevant timescale (150 years). Zero melting could never occur in the real world, since even seawater at the surface freezing temperature would still induce melting at depth. In the deep ice near grounding lines, this means a melting reduction of hundreds of meters per year (Dutrieux et al., 2013; Holland et al., 2023). Under this extreme change, it is reasonable to expect that ice shelves might thicken due to the continued influx of grounded ice, promoting grounding-line re-advance, increased buttressing, and a transition from mass loss to mass gain in the grounded glacier catchment.

This experiment serves two purposes. First, it reveals whether the ice loss is driven by warm present-day ocean conditions, or is a response to historical change. If PIG or TG continue to lose mass despite the complete lack of melting, their ice loss must have a component of adjustment to past change. Second, it reveals whether we can reverse the 20th-century ice loss and recover the expanded pre-1940s ice-sheet state. Zero-melt conditions are a much ‘colder’ climatic forcing than we could ever achieve through policy interventions; if the glaciers fail to re-advance even in this case, reversal is impossible through ocean cooling measures.

## 2. Methods

We conducted zero-melt simulations of the Amundsen Sea Sector for recently-published configurations of the ice-sheet models WAVI (Williams et al., 2025), BISICLES (Trevers et al., 2024) and Úa (Gudmundsson et al., 2023). Each model independently produced zero-melt forward simulations after being initialized into the present-day state (∼2015). This approach allows the robustness of the conclusions to be evaluated over a range of modeling choices. While we focus specifically on the ice response to the removal of ocean forcing for the “standard” versions of these models, we explore additional uncertainties for WAVI and BISICLES. WAVI was used to explore uncertainties in the initial state via the use of alternative regularizations of the ill-posed inverse initialization problem (Arthern & Gudmundsson, 2010), Text S1 in Supporting Information S1. BISICLES was used with one initial state for multiple forward simulations with different values of the critical height above flotation, $h_T$, which represents bed weakening in response to ice thinning (Text S2 in Supporting Information S1). For Úa, a high-resolution initial state was used in a single forward simulation (Text S3 in Supporting Information S1).

### 2.1. WAVI

The WAVI (Wavelet-based Adaptive-grid Vertically-integrated) ice-sheet model is a finite difference model that includes membrane stresses and is vertically integrated but retains the vertical profile of velocity implicitly (Arthern et al., 2015; Bradley et al., 2024; Williams, Arthern, & Bradley, 2026). The equations are solved numerically over a rectangular uniform mesh, with a resolution of 2 km in this study. A subgrid parameterization is used to represent the grounding-line movement on finer scale than the grid resolution by allowing cells to be partially grounded (Arthern & Williams, 2017). We use a Weertman-type sliding law $\tau_b = C|u_b|^{\frac{1}{m}}$, where $\tau_b$ is the basal drag, $u_b$ is the basal velocity, $m$ is a sliding exponent, $m = 3$ and $C$ is athe spatially varying sliding coefficient calculated from the inversion (see below and Text S1 in Supporting Information S1).

The bed topography, ice thickness and surface elevation are provided from the Bedmachine version 3 data set (Morlighem, 2022; Morlighem et al., 2020) but with Pine Island Glacier cavity modified to match sub-shelf bed

10.1029/2026GL122843



topography observations (Dutrieux et al., 2014). WAVI has a fixed ice mask that contains any cells that are fully or partially grounded in the initial state with minimum thickness of 50 m. Since we want to ensure this is a conservative test in which the ice can advance and reground in the region of Thwaites Ice Shelf, any cells within the boundary of TG shelf with $h < 50$ m are prescribed $h = 50$ m $t = 0$ to ensure they are included in the ice mask.

Model initialization is based on data assimilation (Arthern et al., 2015) and is fully described in Text S1 in Supporting Information S1. The inversion produces two-dimensional spatially-varying fields of basal friction coefficient $C$ and dimensionless ice stiffness coefficient $\phi$ that minimize the misfit between simulated and observed surface velocities from MEASURES 2014/15 (Mouginot et al., 2017a), thinning rates from ICESat/ICESat-2 (Smith et al., 2020) and accumulation rates (Arthern et al., 2006). Initial englacial temperatures are provided from the BISICLES ice-sheet model (see Text S2 in Supporting Information S1). Here, we label $d = 1 - \phi$ as 'damage', although we note that this is not strictly just ice damage: this term also captures uncertainties in temperature, impurity content, crystal fabric and grain size. The approximate start date is 2015. $C$ under fully floating ice in the initial state is set as $C = 10^4$ Pa m$^{-1/3}$ a$^{1/3}$, an order of magnitude estimate in broad agreement with $C$ values in the main ice streams.

Since the inversion is an ill-posed problem, we perform multiple inversions with WAVI to explore the sensitivity of the forward simulations to the inverted fields. This is done by varying the inversion parameters ($p$, $q_f$ and $q_g$) that control how much $C$ and $\phi$ can vary from the initial guess (Arthern et al., 2015). This results in different combinations of $C$ and $\phi$ fields, all of which minimize the misfit with observations. Here, default parameters are $p = 0.2$, $q_f = 0.1$ and $q_g = 0.01$, and we present five parameter combinations: $p = 0.2$, $q_f = 0.1$ and $q_g = 0.0$, 0.005, 0.01, 0.02 and $p = 0.1$, $q_f = 0.1$ and $q_g = 0.01$ (see Figures S1 and S2 in Supporting Information S1).

For each initial state, a surface relaxation is performed for 250 years after the initialization procedure, during which the accumulation $a_{\text{relax}}$ is set as $a_{\text{obs}} - \frac{dh}{dt}_{\text{obs}}$. This brings the flux divergence into better agreement with observations of thinning and accumulation (Williams et al., 2025). During the relaxation, ice thickness is not allowed to vary over the shelves, fixing the grounding line in place. This leads to an initialized, relaxed state that is thinning at the observed rate with prescribed 2015 grounding line.

### 2.2. BISICLES

BISICLES (Cornford et al., 2013; Cornford et al., 2025) is a finite-volume ice sheet model which solves the vertically-integrated equations of the L1L2 approximation (Schoof & Hindmarsh, 2010) on a block-structured grid. BISICLES utilizes adaptive mesh refinement to enable a range of mesh resolution from 4 km for slow-flowing inland ice down to 500 m around the grounding line through three levels of refinement.

Our simulations applied a Weertman-type sliding law with additional bed-weakening, $\tau_b = \lambda C|u_b|^{\frac{1}{m}}$ , where $m = 3$. $\lambda$ is the bed-weakening parameter (Joughin et al., 2010), which reduces the basal stress linearly as the ice thins below some critical threshold height-above-flotation, $h_T$

$$\lambda = \begin{cases} \dfrac{(h - h_f)}{\min\left[h_0 - h_f, h_T\right]} & (h - h_f) \le h_T \\ 1 & \text{otherwise,} \end{cases}$$

in which $h$ is the ice thickness, $h_f$ is the flotation thickness and $h_0$ the initial thickness. Including $h_0$ ensures consistency with the initial conditions such that there is no weakening in the initial state. Lambda values only diverge in the simulations with different values of $h_T$ as the ice thickness evolves away from its initial value; there is no shock at the start of the forward simulations (Figure S4 in Supporting Information S1). Simulations were run for $h_T = 0$ m, 100 m, 200 m and 500 m, with a default value of $h_T = 0$ m (see Figure S3 in Supporting Information S1).

Bed topography and ice thickness were provided prior to model initialization from BedMachine version 3 (Morlighem, 2022; Morlighem et al., 2020). The model was initialized through an iterative process of alternating model inversions and periods of relaxation (Text S2 in Supporting Information S1). During the inversions, the basal friction coefficient $C$ and ice stiffening factor φ were optimized to minimize the mismatch to an observed velocity field (Mouginot and Scheuchl, 2019). During relaxation the surface elevation of ice shelves was held fixed while the grounded ice surface was allowed to vary. We applied a surface accumulation rate as the difference between the MAR regional climate model 1980 to 2021 mean (Agosta et al., 2019) and the observed rate of thickness change (Smith et al., 2020) in order to align the flux divergence in the initial state with the observed rate of thinning (van den Akker et al., 2025). Following the final inversion, we extrapolated values of $C$ for floating ice by iteratively applying a convolution to smear out values computed for grounded ice into regions beneath ice shelves.

### 2.3. Úa

We used the version 2024a of ice-flow model Úa to conduct this study (Gudmundsson, 2024). Úa is a finite-element model that solves the shallow ice stream equations (SSA or SSTREAM) on an irregular triangular mesh. Various criteria can be applied to automatically adapt the mesh for resolution requirements at defined locations, such as near the grounding line, calving front, or locations experiencing high strain rates. Mesh resolution ranges from 8 km in slow-flowing inland regions to 500 m around the grounding line. The ice-flow model solves the momentum and mass conservation equations simultaneously using implicit time integration with respect to both ice velocities and ice thickness. In all numerical results presented, the computational domain was discretized using linear 3-node triangular elements.

The simulations are initialized with the present-day geometry (Morlighem et al., 2020) and surface velocities (Rignot et al., 2011). The Weertman sliding law (Weertman, 1957) with $m = 3$ is used for basal sliding, and Glen's flow law with $n = 3$ is used for ice deformation. The rate factor in Glen's flow law and the basal slipperiness parameter in Weertman sliding law are optimized using an adjoint method to ensure the observed velocity field and the observed ice thickness changes (Nilsson et al., 2023) are reproduced by the model (see Text S3 in Supporting Information S1). Basal slipperiness parameters are estimated for existing grounded ice and linearly extrapolated across newly grounded regions that result from grounding line advance.

### 2.4. Forward Model Simulations

For all of the simulations in this study, we assume no sub-ice-shelf melting throughout each 150-year simulation. WAVI uses constant accumulation rates (Arthern et al., 2006), BISICLES used the MAR regional climate model 1980 to 2021 mean surface accumulation rate (Agosta et al., 2019), and Úa used constant surface mass balance from regional model RACMO2.3 output for 1979–2023 (Noel et al., 2023). These present-day forcings and the spatially-varying fields of damage/ice stiffness and basal friction coefficients were held constant. Ice fronts were kept fixed in WAVI and Úa, and were allowed to retreat through thinning but not advance in BISICLES.

### 2.5. Current Rates of Ice Loss

Estimates of current rates of ice loss in terms of SLC (mm/year) are calculated from thinning data for 2003–2019 (Smith et al., 2020). Specifically, rates of change of thickness over grounded ice were used to estimate the total SLC per year separately for each glacier catchment. This gave 0.16 mm/year for PIG and 0.11 mm/year for TG.

## 3. Results

Figure 1 shows the grounding-line changes for three default simulations, while Figure 2 shows the evolution of cumulative sea level contribution (SLC) for all simulations. Under zero-melt conditions, for all simulations over all three models, PIG rapidly readvances to the prominent sea-bed ridge on which it was grounded prior to the 1940s (Reed et al., 2024; Smith et al., 2017) (Figures 1b–1d). PIG's mass gain is clearly shown in Figures 2a–2c, where negative SLC indicates mass gain. PIG switches from mass loss to mass gain rapidly, within 7 years for all simulations (Figures 2d–2f), and is still gaining mass after 150 years. This behavior is as expected, after the significant mass loss from ice-shelf melting (Dutrieux et al., 2013) is removed.

The behavior of TG is starkly different: For all simulations, TG continues to lose mass over the next 150 years, despite the cessation of ice-shelf melt, and irrespective of modeling choices (Figures 2g–2i). No simulation shows significant advance of the main grounding line of Thwaites (Figures 1 and 1e–1g). Rates of SLC decline in all simulations (Figures 2j–2l), at different rates for each model due to modeling choices (see Section 2). This decaying rate of ice loss could indicate TG is nearing a new steady state (Hill et al., 2023), distinct from the initial

10.1029/2026GL122843

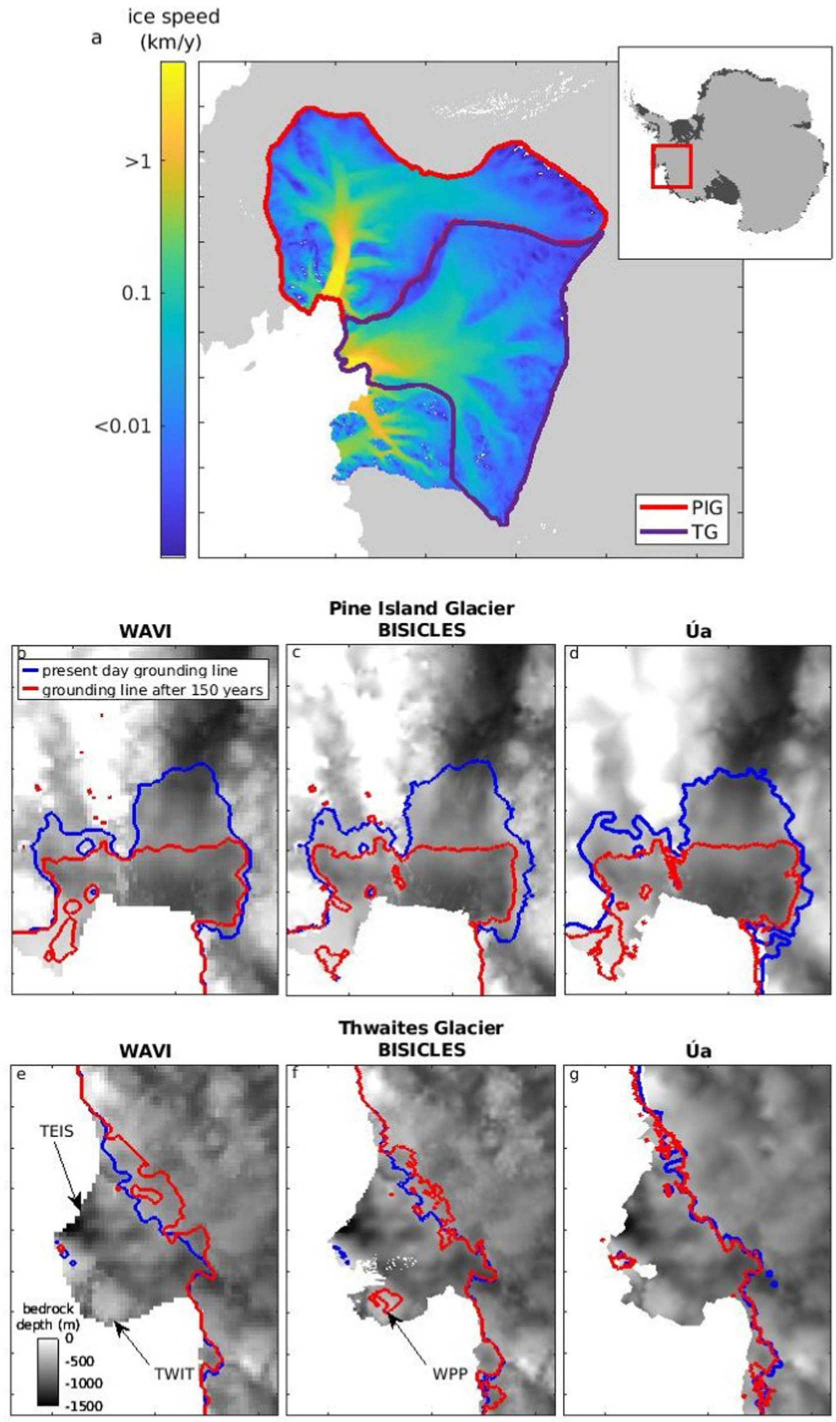


**Figure 1.** Contrasting grounding-line response of PIG and Thwaites in hypothetical zero-melt scenario. (a) Model domain and catchment basins for PIG (red), TG (purple) (Mouginot et al., 2017b). Colors show an example of initialized present-day surface velocities from the WAVI ice-sheet model for default parameters ($p = 0.2$, $q_g = 0.01$, $q_f = 0.1$). (b–g) Initial grounding line position (blue) and position after 150 years (red) for each ice sheet model with each model's default parameters (see Methods). Bed topography is shown in greyscale. TEIS: Thwaites Eastern Ice Shelf, TWIT: Thwaites Western Ice Tongue, WPP: Western Pinning Point.

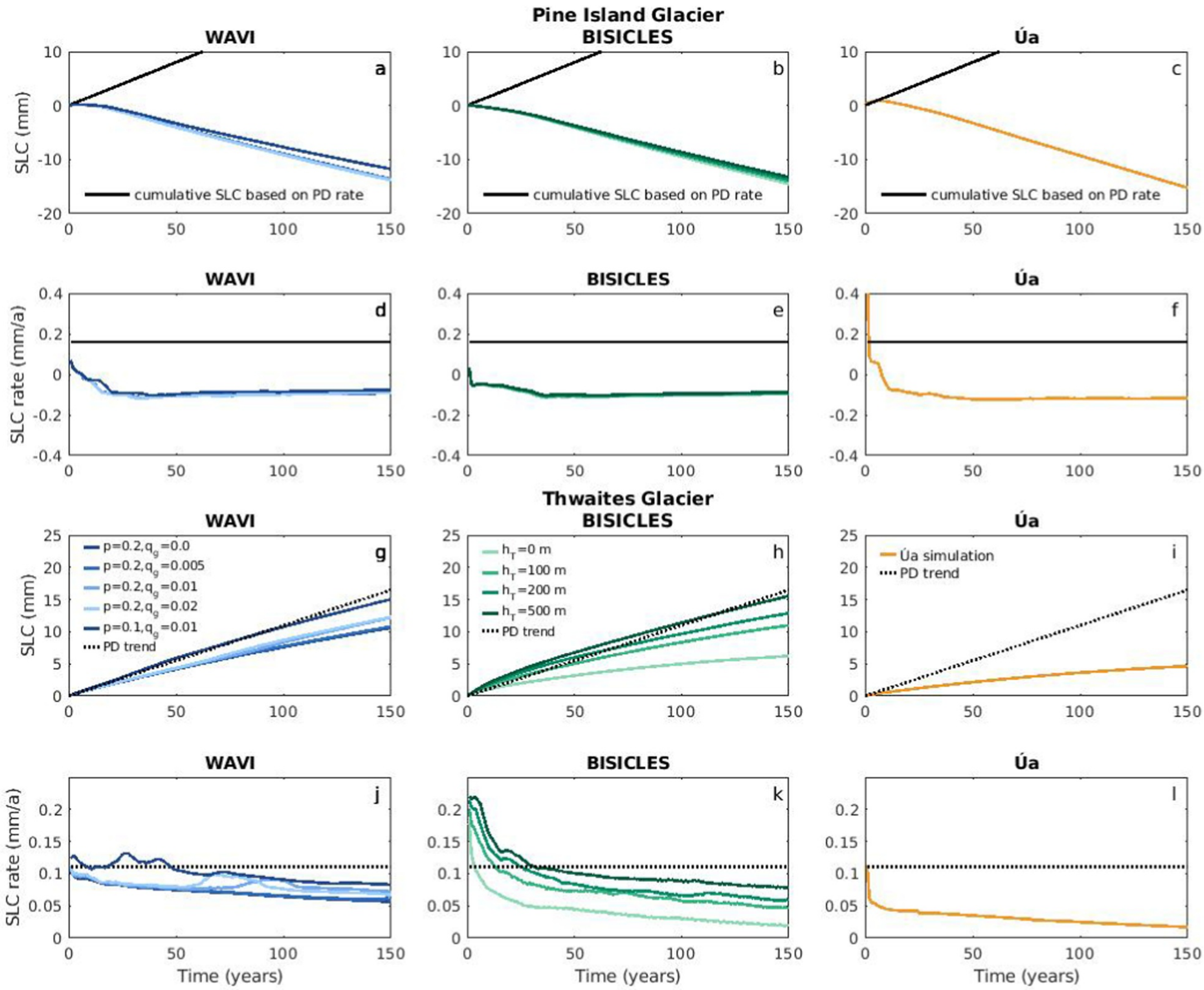


**Figure 2.** Contrasting PIG and Thwaites sea-level contributions in zero-melt scenario. Cumulative sea-level contribution (SLC) and the associated rate of SLC for all three ice sheet models for PIG and TG. Black lines show the current (PD, present day) rate of SLC (dotted) for each glacier (Smith et al., 2020) and the cumulative SLC (solid) assuming this constant rate over the next 150 years. For WAVI, different blue shades indicate different initial states (dark to light: $p = 0.2$ and $q_g = 0.0, 0.005, 0.01, 0.02$, darkest blue indicates $p = 0.1$, $q_f = 0.1$, and $q_g = 0.01$ in all simulations). For BISICLES, increases in critical height above flotation, $h_T$, are shown through progressively darker greens ($h_T = 0$ m, 100 m, 200 m, 500 m).

2015 state. It is remarkable that ice loss continues for over a century despite the removal of the significant mass sink from melting (Holland et al., 2023).

Our ensemble of model simulations display variability in mass loss from TG. This is not unexpected since the models used different initialization procedures and different data sets and model parameters, and modeled inverted fields differ (Figures S1, S2, and S5–S8 in Supporting Information S1). While all three inversions use observations to minimize the misfit with present-day thinning rates, this does not imply thinning will persist indefinitely at this rate in the simulations. In fact, PIG switches to mass gain with 7 years and our simulations are all in strong agreement. For TG, we find a larger spread of SLC, highlighting Thwaites as a source of uncertainty in mass-loss projections (Seroussi et al., 2023). Despite these differences, the simulations show the same qualitative behavior of mass loss for TG and mass gain for PIG.

Figure 3 shows thickness changes over 100 years of simulation for three default simulations under no ocean melt. All three model simulations show significant thickening over PIG's main trunk and ice shelf, in contrast to widespread thinning along the main trunk of TG. Over TG's ice shelf, the pattern of thickness change is more complex. Thickening of the TWIT and re-pinning on the Western pinning point occurs in the BISICLES

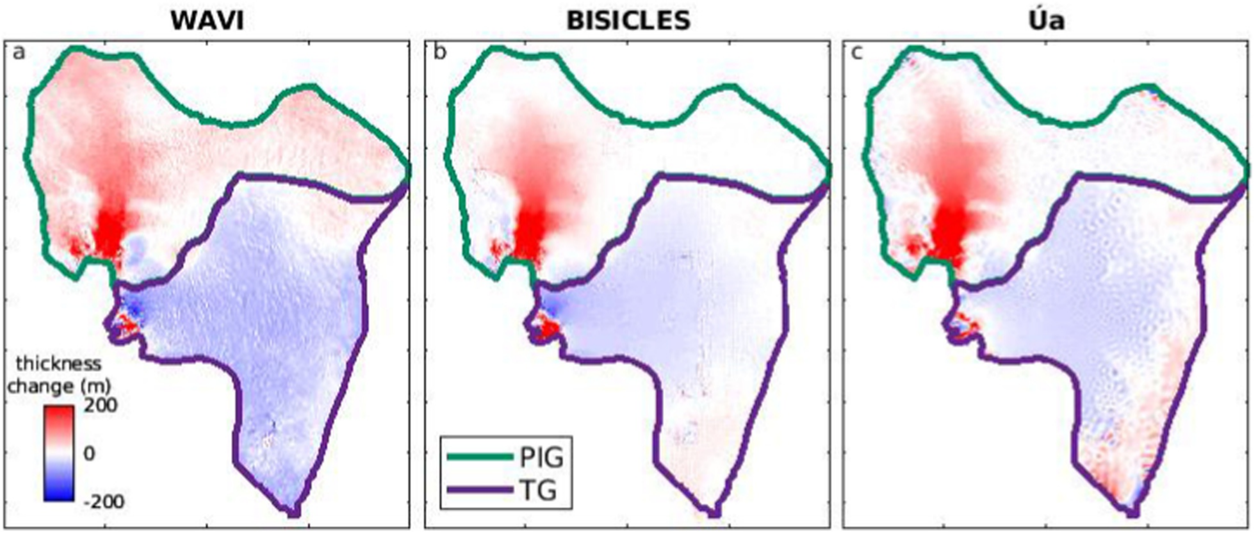


**Figure 3.** Contrasting thickness changes to PIG and TG in hypothetical zero-melt scenario. (a–c) Thickness change to PIG (green) and TG (purple) catchements over after 100 simulation years for each ice sheet model with each model's default parameters (as in Figure 1). Positive (red) indicates mass gain and negative (blue) indicates mass loss.

simulations due to unpinning from the Eastern pinning point and subsequent deflection of ice flow away from TEIS (Figures 1f and 3b). However, this does not halt the ice loss since the ice in the TWIT is weakened in this simulation (shown by a decrease in ice stiffness factor $\varphi$ from the inversion, Figure S5 in Supporting Information S1), so re-pinning provides only minimal additional buttressing (Figure 2h). For WAVI and Úa, some thickening of TWIT occurs but this is insufficient to re-ground on the Western pinning point (Figures 1e–1g and 3a–3c). TEIS maintains a reduced pinning point in WAVI (Figure 1e) and an increased pinning point in Úa (Figure 1g), but both are insufficient to significantly readvance the grounding line in Thwaites' Eastern region. Indeed, TEIS has been found to provide limited buttressing to grounded ice in TG's present-day state (Gudmundsson et al., 2023).

## 4. Discussion

The results of this simple experiment show a remarkable contrast in the response of PIG and TG to the removal of sub-ice-shelf melting. These simulations are not intended to predict the future of these glaciers or to explore the full space of modeling choices. Instead, they provide insight into the drivers and potential reversibility of their ongoing ice loss by exploring the response to an extreme hypothetical ocean forcing. For PIG, current ice loss can be reversed by removing the ocean forcing alone (Reed et al., 2024). For TG, ice loss continues and the glacier does not return to its advanced pre-1940s state after 150 years of zero sub-ice-shelf melting (Bett et al., 2024). Thus, we conclude that TG exhibits a component of ice loss that is not driven by warm ocean conditions in the present day. This demonstrates that TG's current mass loss is, at least in part, an ongoing transient response to historical forcing (Clark et al., 2024; Gudmundsson et al., 2023; Joughin et al., 2014; O'Connor et al., 2023; Smith et al., 2017). This is a clear result because zero melting is such an extreme scenario, and is robust across three independent ice-sheet models.

For TG, the rate of ice loss in these experiments does not grow over time; rather, it decreases over the 150-year simulations. Thus, under this extreme hypothetical scenario of zero oceanic melt we do not find evidence of self-reinforcing feedbacks leading to accelerating future ice loss. However, these simulations do not rule out the possibility of such ever-growing feedbacks, or additional ice loss driven by historical ocean warming, because zero melt is such an extreme scenario. Further work is needed to assess these components of the ongoing and future ice loss under more realistic, non-zero ocean forcing scenarios.

It is worth considering why TG cannot regrow. TG could advance if TWIT re-grounded on its western pinning point and gained significant buttressing, as PIG does. BISICLES does reground in this area (Figure 1f) but does not gain sufficient buttressing to prevent ice loss, due to the weakening/damage of the TG ice shelf that is

10.1029/2026GL122843

initialized in our models. WAVI and Úa do not even re-ground in this area because TWIT spreads and thins too rapidly after the ice crosses the grounding line. Thus, the retreat of TG has led to a present-day state that cannot re-advance to recover the pre-1940s state over the next 150 years through any changes in ocean melt.

It is possible that in this extreme scenario "healing", through the influx of intact ice into the shelf in the future, is a mechanism to decrease ice-shelf damage and increase buttressing (Surawy-Stepney, Hogg, Cornford, & Davison, 2023). However, the present-day state of the ice upstream of TG's grounding line currently shows significant damage (Surawy-Stepney, Hogg, Cornford, & Hogg, 2023). The chain of processes by which the ice shelf could thicken and potentially lead to decreased damage formation inland, and thus advection of intact ice into the shelf, is a complex question. Including damage evolution in regional models is still a developing area of research (Sun et al., 2017), and there is great uncertainty in the physical representation of the processes (Li et al., 2025). A key feature of our study is that it reveals the grave implications of the present-day ice state, which includes its damage, and so we preserve the present-day damage to illustrate that point. Using a damage evolution model is beyond the scope of this study, but should be an active area of future research.

Previous studies explore whether these glaciers are 'unstable' or have already 'passed a tipping point' that would commit the system to accelerating and potentially irreversible future retreat. It has been suggested that PIG is "probably" already engaged in an unstable retreat (Favier et al., 2014), and has the potential to pass multiple 'tipping points' if ocean warming continues (Rosier et al., 2021). For TG, while some modeling studies find strong evidence that marine ice-sheet destabilization is already under way (Joughin et al., 2014), or that a tipping point may have been passed (Bett et al., 2024), other analyses suggest that TG's present-day grounding line retreat is not irreversible or self-sustained yet (Gudmundsson et al., 2023; Hill et al., 2023) and irreversible collapse is not yet inevitable (Reese et al., 2023).

Here, we do not assess the long-term future stability of PIG and TG. Instead, we show that historical ice loss from TG may not be reversible through reductions in ocean forcing alone over policy-relevant timescales. TG had a larger ice volume in the past (Clark et al., 2024) under conditions that must have included significant ice shelf melting. A past perturbation in melt triggered a retreat of TG since the mid twentieth century (Clark et al., 2024; Holland et al., 2022; O'Connor et al., 2023), but we find the glacier does not return to its expanded pre-1940s state even in a much 'colder' state with zero melting over 150 years; no melt perturbation can lead to TG's recovery on the same timescale as the retreat (Bett et al., 2026). This suggests that TG has passed some kind of system threshold separating the historical and present-day states of TG. Formally determining whether this threshold constitutes a 'tipping point' would require a broader suite of stability and reversibility experiments with a coupled ice-ocean model. The historical threshold proposed here separates the expanded pre-1940s historical configuration from the present-day state but does not imply that any future retreat will be irreversible. We find no evidence for such behavior in our simulations, but note that accelerating rates of ice loss and/or irreversible future retreat could occur under more realistic ocean forcing and cannot be ruled out by our zero-melt experiments.

Our simulations over three independent models indicate that Thwaites Glacier will continue to lose ice for the next 150 years under any future melt scenario. This suggests that some future sea-level contribution is unavoidable on centennial timescales, even under strong policy interventions that result in ocean cooling. In fact, future ocean warming appears unavoidable on century timescales (Naughten et al., 2023), and overall ice loss from this region is strongly dependent on the future trajectory of ocean temperatures (Bett et al., 2024). Further work is required to reduce uncertainties in projections of ice loss from TG in particular (Seroussi et al., 2023). Mitigation of greenhouse-gas emissions to minimize the rate of ice loss from this region remains essential to avoid significant future sea-level rise from West Antarctica.

## 5. Conclusions

This study assesses whether the present-day ice loss from Pine Island and Thwaites glaciers is driven by ongoing ocean forcing or the response to a historical perturbation. We remove ocean forcing in three ice-sheet models by setting sub-ice-shelf melt to zero, finding that PIG thickens and re-advances, whereas TG continues to lose ice (at a decaying rate). Thus, we conclude that the ice loss from TG must have a substantial component that is an ongoing transient response to historical forcing. Furthermore, we find that the historical retreat of TG has led to a present-day state that does not re-advance under any ocean cooling measures; Thwaites is now in a qualitatively different system state to its 1940s configuration. While this does not imply commitment to accelerating future retreat, the present-day mass loss trend from Thwaites may not be reversed through reductions in ocean forcing alone; some future sea-level contribution is unavoidable. Thus, our results highlight the need for policy responses that combine adaptation to the sea-level contribution that is inevitable with mitigation of greenhouse gas emissions to minimize the total rate.

## Conflict of Interest

The authors declare no conflicts of interest relevant to this study.

## Availability Statement

The model outputs for the set of ice-sheet model simulations presented in this study can be found at https://zenodo.org/records/21485345 (Williams, Sun, Trevers, 2026). The version of WAVI used in this study is documented in Williams, Arthern, & Bradley (2026). GitHub: Cornford et al. (2025) and Gudmundsson (2024).

**Acknowledgments**

C. R. W., M. T., S. S., P. R. H. and R. J. A. were partly funded by ISOTIPIC (UKRI-NERC: Grant NE/Z503344/1). C. R. W., A. T. B. and R. J. A. were partly funded by IceDice (UKRI-NERC: Grant UKRI1276). Initial work by C. R. W., R. J. A. and P. R. H. was funded through the MELT project, a component of the International Thwaites Glacier Collaboration (ITGC). Support from National Science Foundation (NSF: Grant 1739003) and Natural Environment Research Council (NERC: Grant NE/S006656/1). Logistics provided by NSF-U.S. Antarctic Program and NERC-British Antarctic Survey. ITGC Contribution No. ITGC-164.

## References

Agosta, C., Amory, C., Kittel, C., Orsi, A., Favier, V., Gallée, H., et al. (2019). Estimation of the Antarctic surface mass balance using the regional climate model MAR (1979–2015) and identification of dominant processes. *The Cryosphere*, *13*(1), 281–296. https://doi.org/10.5194/tc-13-281-2019

Alley, K. E., Wild, C. T., Luckman, A., Scambos, T. A., Truffer, M., Pettit, E. C., et al. (2021). Two decades of dynamic change and progressive destabilization on the Thwaites Eastern Ice Shelf. *The Cryosphere*, *15*(11), 5187–5203. https://doi.org/10.5194/tc-15-5187-2021

Arthern, R. J., & Gudmundsson, G. H. (2010). Initialization of ice-sheet forecasts viewed as an inverse Robin problem. *Journal of Glaciology*, *56*(197), 527–533. https://doi.org/10.3189/002214310792447699

Arthern, R. J., Hindmarsh, R. C. A., & Williams, C. R. (2015). Flow speed within the Antarctic ice sheet and its controls inferred from satellite observations. *Journal of Geophysical Research: Earth Surface*, *120*(7), 1171–1188. https://doi.org/10.1002/2014JF003239

Arthern, R. J., & Williams, C. R. (2017). The sensitivity of West Antarctica to the submarine melting feedback. *Geophysical Research Letters*, *44*(5), 2352–2359. https://doi.org/10.1002/2017GL072514

Arthern, R. J., Winebrenner, D. P., & Vaughan, D. G. (2006). Antarctic snow accumulation mapped using polarization of 4.3-cm wavelength microwave emission. *Journal of Geophysical Research*, *111*(D6). https://doi.org/10.1029/2004JD005667

Bett, D. T., Bradley, A. T., Miles, B. W. J., Williams, C. R., Holland, P. R., & Arthern, R. J. (2026). *Modelling the evolution of Thwaites Glacier over the 20th century* (Vol. 2026, pp. 1–43). EGUsphere. https://doi.org/10.5194/egusphere-2026-669

Bett, D. T., Bradley, A. T., Williams, C. R., Holland, P. R., Arthern, R. J., & Goldberg, D. N. (2024). Coupled ice–ocean interactions during future retreat of West Antarctic ice streams in the Amundsen Sea sector. *The Cryosphere*, *18*(6), 2653–2675. https://doi.org/10.5194/tc-18-2653-2024

Bett, D. T., Holland, P. R., Naveira Garabato, A. C., Jenkins, A., Dutrieux, P., Kimura, S., & Fleming, A. (2020). The impact of the Amundsen Sea freshwater balance on ocean melting of the West Antarctic ice sheet. *Journal of Geophysical Research: Oceans*, *125*(9), e2020JC016305. https://doi.org/10.1029/2020JC016305

Bradley, A. T., Arthern, R. J., Bett, D. T., Williams, C. R., & Byrne, J. (2024). WAVI.jl: Ice sheet modelling in julia. *Journal of Open Source Software*, *9*(95), 5584. https://doi.org/10.21105/joss.05584

Clark, R. W., Wellner, J. S., Hillenbrand, C.-D., Totten, R. L., Smith, J. A., Miller, L. E., et al. (2024). Synchronous retreat of Thwaites and Pine Island glaciers in response to external forcings in the presatellite era. *Proceedings of the National Academy of Sciences*, *121*(11), e2211711120. https://doi.org/10.1073/pnas.2211711120

Cornford, S. L., Martin, D. F., Graves, D. T., Ranken, D. F., Le Brocq, A. M., Gladstone, R. M., et al. (2013). Adaptive mesh, finite volume modeling of marine ice sheets. *Journal of Computational Physics*, *232*(1), 529–549. https://doi.org/10.1016/j.jcp.2012.08.037

Cornford, S. L. a. M., D, F., Trevers, M., Kachuck, S. B., Mitcham, T., Adams, M., et al. (2025). Release of BISICLES used in this study. *Zenodo*. [Software]. https://doi.org/10.5281/zenodo.17817189

Dutrieux, P., De Rydt, J., Jenkins, A., Holland, P. R., Ha, H. K., Lee, S. H., et al. (2014). Strong sensitivity of pine Island ice-shelf melting to climatic variability. *Science*, *343*(6167), 174–178. https://doi.org/10.1126/science.1244341

Dutrieux, P., Vaughan, D. G., Corr, H. F. J., Jenkins, A., Holland, P. R., Joughin, I., & Fleming, A. H. (2013). Pine Island glacier ice shelf melt distributed at kilometre scales. *The Cryosphere*, *7*(5), 1543–1555. https://doi.org/10.5194/tc-7-1543-2013

Favier, L., Durand, G., Cornford, S. L., Gudmundsson, G. H., Gagliardini, O., Gillet-Chaulet, F., et al. (2014). Retreat of Pine Island Glacier controlled by marine ice-sheet instability. *Nature Climate Change*, *4*(2), 117–121. https://doi.org/10.1038/nclimate2094

Gudmundsson, G. H., Barnes, J. M., Goldberg, D. N., & Morlighem, M. (2023). Limited impact of thwaites ice Shelf on future ice loss from Antarctica. *Geophysical Research Letters*, *50*(11), e2023GL102880. https://doi.org/10.1029/2023GL102880

Gudmundsson, H. (2024). GHilmarG/UaSource: Ua2024a. *Zenodo*. [Software]. https://doi.org/10.5281/zenodo.11394406

Hill, E. A., Urruty, B., Reese, R., Garbe, J., Gagliardini, O., Durand, G., et al. (2023). The stability of present-day Antarctic grounding lines – Part 1: No indication of marine ice sheet instability in the current geometry. *The Cryosphere*, *17*(9), 3739–3759. https://doi.org/10.5194/tc-17-3739-2023

Holland, P. R., Bevan, S. L., & Luckman, A. J. (2023). Strong Ocean melting feedback during the recent retreat of thwaites Glacier. *Geophysical Research Letters*, *50*(8), e2023GL103088. https://doi.org/10.1029/2023GL103088

Holland, P. R., Bracegirdle, T. J., Dutrieux, P., Jenkins, A., & Steig, E. J. (2019). West Antarctic ice loss influenced by internal climate variability and anthropogenic forcing. *Nature Geoscience*, *12*(9), 718–724. https://doi.org/10.1038/s41561-019-0420-9

Holland, P. R., O'Connor, G. K., Bracegirdle, T. J., Dutrieux, P., Naughten, K. A., Steig, E. J., et al. (2022). Anthropogenic and internal drivers of wind changes over the Amundsen Sea, West Antarctica, during the 20th and 21st centuries. *The Cryosphere*, *16*(12), 5085–5105. https://doi.org/10.5194/tc-16-5085-2022

Joughin, I., Smith, B. E., & Holland, D. M. (2010). Sensitivity of 21st century sea level to ocean-induced thinning of Pine Island Glacier, Antarctica. *Geophysical Research Letters*, *37*(20). https://doi.org/10.1029/2010gl044819

Joughin, I., Smith, B. E., & Medley, B. (2014). Marine ice sheet collapse potentially under way for the thwaites Glacier Basin, West Antarctica. *Science*, *344*(6185), 735–738. https://doi.org/10.1126/science.1249055

Lhermitte, S., Sun, S., Shuman, C., Wouters, B., Pattyn, F., Wuite, J., et al. (2020). Damage accelerates ice shelf instability and mass loss in Amundsen Sea Embayment. *Proceedings of the National Academy of Sciences*, *117*(40), 24735–24741. https://doi.org/10.1073/pnas.1912890117

Li, Y., Coulon, V., Blasco, J., Qiao, G., Yang, Q., & Pattyn, F. (2025). Damage intensity increases ice mass loss from Thwaites Glacier, Antarctica. *The Cryosphere*, *19*(10), 4373–4390. https://doi.org/10.5194/tc-19-4373-2025

Mawbey, E. M., Smith, J. A., Hillenbrand, C. D., Hendry, K. R., McClymont, E. L., Greaves, M. J., et al. (2026). Ocean heat forced West Antarctic Ice Sheet retreat after the Last Glacial Maximum. *Nature Communications*, *17*(1), 2079. https://doi.org/10.1038/s41467-026-68949-5

Morlighem, M. (2022). MEaSUREs BedMachine Antarctica (version 3). *NASA National Snow and Ice Data Center Distributed Active Archive Center*. [Dataset]. https://doi.org/10.5067/FPSU0V1MWUB6

Morlighem, M., Rignot, E., Binder, T., Blankenship, D., Drews, R., Eagles, G., et al. (2020). Deep glacial troughs and stabilizing ridges unveiled beneath the margins of the Antarctic ice sheet. *Nature Geoscience*, *13*(2), 132–137. https://doi.org/10.1038/s41561-019-0510-8

Mouginot, J., Rignot, E., & Scheuchl, B. (2014). Sustained increase in ice discharge from the Amundsen Sea embayment, West Antarctica, from 1973 to 2013. *Geophysical Research Letters*, *41*(5), 1576–1584. https://doi.org/10.1002/2013GL059069

Mouginot, J., Scheuchl, B., & Rignot, E. (2017a). MEaSUREs annual antarctic ice velocity maps (Version 1). *NASA National Snow and Ice Data Center Distributed Active Archive Center*. [Dataset]. https://doi.org/10.5067/9T4EPQXTJYW9

Mouginot, J., Scheuchl, B., & Rignot, E. (2017b). MEaSUREs antarctic boundaries for IPY 2007-2009 from satellite radar (version 2). *NASA National Snow and Ice Data Center Distributed Active Archive Center*. [Dataset]. https://doi.org/10.5067/AXE4121732AD

Mouginot, J. A. R. E., & Scheuchl, B. (2019). MEaSUREs phase-based Antarctica ice velocity map (version 1). *NASA National Snow and Ice Data Center Distributed Active Archive Center*. [Dataset]. https://doi.org/10.5067/PZ3NJ5RXRH10

Naughten, K. A., Holland, P. R., & De Rydt, J. (2023). Unavoidable future increase in West Antarctic ice-shelf melting over the twenty-first century. *Nature Climate Change*, *13*(11), 1222–1228. https://doi.org/10.1038/s41558-023-01818-x

Naughten, K. A., Holland, P. R., Dutrieux, P., Kimura, S., Bett, D. T., & Jenkins, A. (2022). Simulated twentieth-century ocean warming in the Amundsen Sea, West Antarctica. *Geophysical Research Letters*, *49*(5), e2021GL094566. https://doi.org/10.1029/2021GL094566

Nilsson, J., Gardner, A., & Paolo, F. (2023). MEaSUREs ITS_LIVE antarctic grounded ice sheet elevation change (version 1). *NASA National Snow and Ice Data Center Distributed Active Archive Center*. [Dataset]. https://doi.org/10.5067/L3LSVDZS15ZV

Noel, B., van Wessem, J. M., Wouters, B., Trusel, L., Lhermitte, S., & van den Broeke, M. R. (2023). Higher Antarctic ice sheet accumulation and surface melt rates revealed at 2 km resolution. *Nature Communications*, *14*(1), 7949. https://doi.org/10.1038/s41467-023-43584-6

O'Connor, G. K., Holland, P. R., Steig, E. J., Dutrieux, P., & Hakim, G. J. (2023). Characteristics and rarity of the strong 1940s westerly wind event over the Amundsen Sea, West Antarctica. *The Cryosphere*, *17*(10), 4399–4420. https://doi.org/10.5194/tc-17-4399-2023

Reed, B., Green, J. A. M., Jenkins, A., & Gudmundsson, G. H. (2024). Recent irreversible retreat phase of Pine Island Glacier. *Nature Climate Change*, *14*(1), 75–81. https://doi.org/10.1038/s41558-023-01887-y

Reese, R., Garbe, J., Hill, E. A., Urruty, B., Naughten, K. A., Gagliardini, O., et al. (2023). The stability of present-day Antarctic grounding lines – Part 2: Onset of irreversible retreat of Amundsen Sea glaciers under current climate on centennial timescales cannot be excluded. *The Cryosphere*, *17*(9), 3761–3783. https://doi.org/10.5194/tc-17-3761-2023

Rignot, E., Mouginot, J., & Scheuchl, B. (2011). Ice flow of the Antarctic ice sheet. *Science*, *333*(6048), 1427–1430. https://doi.org/10.1126/science.1208336

Rignot, E., Mouginot, J., Scheuchl, B., van den Broeke, M., van Wessem, M. J., & Morlighem, M. (2019). Four decades of Antarctic Ice Sheet mass balance from 1979–2017. *Proceedings of the National Academy of Sciences*, *116*(4), 1095–1103. https://doi.org/10.1073/pnas.1812883116

Rosier, S. H. R., Reese, R., Donges, J. F., De Rydt, J., Gudmundsson, G. H., & Winkelmann, R. (2021). The tipping points and early warning indicators for Pine Island Glacier, West Antarctica. *The Cryosphere*, *15*(3), 1501–1516. https://doi.org/10.5194/tc-15-1501-2021

Schoof, C., & Hindmarsh, R. C. A. (2010). Thin-Film flows with Wall slip: An asymptotic analysis of higher order Glacier flow models. *The Quarterly Journal of Mechanics and Applied Mathematics*, *63*(1), 73–114. https://doi.org/10.1093/qjmam/hbp025

Seroussi, H., Verjans, V., Nowicki, S., Payne, A. J., Goelzer, H., Lipscomb, W. H., et al. (2023). Insights into the vulnerability of Antarctic glaciers from the ISMIP6 ice sheet model ensemble and associated uncertainty. *The Cryosphere*, *17*(12), 5197–5217. https://doi.org/10.5194/tc-17-5197-2023

Shepherd, A., Gilbert, L., Muir, A. S., Konrad, H., McMillan, M., Slater, T., et al. (2019). Trends in antarctic ice sheet elevation and mass. *Geophysical Research Letters*, *46*(14), 8174–8183. https://doi.org/10.1029/2019GL082182

Shepherd, A., Wingham, D., & Rignot, E. (2004). Warm ocean is eroding West Antarctic ice sheet. *Geophysical Research Letters*, *31*(23). https://doi.org/10.1029/2004gl021106

Smith, B., Fricker, H. A., Gardner, A. S., Medley, B., Nilsson, J., Paolo, F. S., et al. (2020). Pervasive ice sheet mass loss reflects competing ocean and atmosphere processes. *Science*, *368*(6496), 1239–1242. https://doi.org/10.1126/science.aaz5845

Smith, J. A., Andersen, T. J., Shortt, M., Gaffney, A. M., Truffer, M., Stanton, T. P., et al. (2017). Sub-ice-shelf sediments record history of twentieth-century retreat of Pine Island Glacier. *Nature*, *541*(7635), 77–80. https://doi.org/10.1038/nature20136

Steig, E. J., Ding, Q., Battisti, D. S., & Jenkins, A. (2012). Tropical forcing of circumpolar deep water inflow and outlet glacier thinning in the Amundsen Sea embayment, West Antarctica. *Annals of Glaciology*, *53*(60), 19–28. https://doi.org/10.3189/2012AoG60A110

Sun, S., Cornford, S. L., Moore, J. C., Gladstone, R., & Zhao, L. (2017). Ice shelf fracture parameterization in an ice sheet model. *The Cryosphere*, *11*(6), 2543–2554. https://doi.org/10.5194/tc-11-2543-2017

Surawy-Stepney, T., Hogg, A. E., Cornford, S. L., & Davison, B. J. (2023). Episodic dynamic change linked to damage on the Thwaites Glacier Ice Tongue. *Nature Geoscience*, *16*(1), 37–43. https://doi.org/10.1038/s41561-022-01097-9

Surawy-Stepney, T., Hogg, A. E., Cornford, S. L., & Hogg, D. C. (2023). Mapping Antarctic crevasses and their evolution with deep learning applied to satellite radar imagery. *The Cryosphere*, *17*(10), 4421–4445. https://doi.org/10.5194/tc-17-4421-2023

Trevers, M., Cornford, S. L., Payne, A. J., Gasson, E., & Bevan, S. L. (2024). Retreat of Thwaites Glacier triggered by its Neighbours [preprint]. *ESS Open Archive*. https://doi.org/10.22541/essoar.170957499.97583808/v1

van den Akker, T., Lipscomb, W. H., Leguy, G. R., Bernales, J., Berends, C. J., van de Berg, W. J., & van de Wal, R. S. W. (2025). Present-day mass loss rates are a precursor for West Antarctic Ice Sheet collapse. *The Cryosphere*, *19*(1), 283–301. https://doi.org/10.5194/tc-19-283-2025

Weertman, J. (1957). On the sliding of glaciers. *Journal of Glaciology*, *3*(21), 33–38. https://doi.org/10.3189/s0022143000024709

Williams, C. R., Arthern, R. J., & Bradley, A. T. (2026). WAVI.jl-Williams2026: Release of WAVI used for Williams et al 2026 GRL [Software]. *Zenodo*. https://doi.org/10.5281/ZENODO.21444845

Williams, C. R., Sun, S., & Trevers, M. (2026). Model outputs for Amundsen Sea sector of West Antarctica under zero ocean melting. *Zenodo*. [Dataset]. https://doi.org/10.5281/zenodo.21485345

Williams, C. R., Thodoroff, P., Arthern, R. J., Byrne, J., Hosking, J. S., Kaiser, M., et al. (2025). Calculations of extreme sea level rise scenarios are strongly dependent on ice sheet model resolution. *Communications Earth & Environment*, *6*(1), 60. https://doi.org/10.1038/s43247-025-02010-z

## References From the Supporting Information

Bevan, S., Cornford, S. L., Gilbert, L., Otosaka, I., Martin, D., & Surawy-Stepney, T. (2023). Amundsen Sea Embayment ice-sheet mass-loss predictions to 2050 calibrated using observations of velocity and elevation change. *Journal of Glaciology*, *69*(278), 1–11. https://doi.org/10.1017/jog.2023.57

Burton-Johnson, A., Dziadek, R., & Martin, C. (2020). Review article: Geothermal heat flow in Antarctica: Current and future directions. *The Cryosphere*, *14*(11), 3843–3873. https://doi.org/10.5194/tc-14-3843-2020

Cornford, S. L., Martin, D. F., Payne, A. J., Ng, E. G., Le Brocq, A. M., Gladstone, R. M., et al. (2015). Century-scale simulations of the response of the West Antarctic Ice Sheet to a warming climate. *The Cryosphere*, *9*(4), 1579–1600. https://doi.org/10.5194/tc-9-1579-2015

Gardner, A. S., Fahnestock, M., Greene, C. A., Kennedy, J. H., Liukis, M., López, L. A., & Scambos, T. (2025). MEaSUREs ITS_LIVE regional Glacier and ice sheet surface velocities. (NSIDC-0776, version 2).